Contents lists available at ScienceDirect

Construction and Building Materials

journal homepage: www.elsevier.com/locate/conbuildmat

Dispersing performance of different kinds of polycarboxylate (PCE) superplasticizers in cement blended with a calcined clay

Marlene Schmid, Johann Plank *

Technical University of Munich, Department of Chemistry, Chair for Construction Chemistry, Lichtenbergstraße 4, 85748 Garching, Germany

HIGHLIGHTS

- A calcined clay (CC) rich in meta illite and smectite was used as SCM.
- CC increased the water demand of the composite cements considerably.
- At 50% clinker substitution, PCE dosages increased by ~100% compared to OPC.
- Methallyl ether (HPEG)-based PCEs were found most effective in both cement and CC.
- Adsorption measurements suggest PCE interaction with OPC stronger than with CC.

GRAPHICAL ABSTRACT
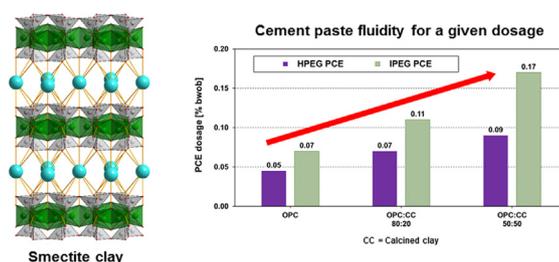
Adapted from: Gournis et al., A neutron diffraction study of alkali cation migration in montmorillonites, Phys Chem Minerals 35 (2008) 49-58; visualized with Diamond software (Version 3.2).

ABSTRACT

This study investigates the dispersing effectiveness of purposely selected methacrylate ester (MPEG), iso-prenol ether (IPEG) and methallyl ether (HPEG) based polycarboxylate (PCE) superplasticizers of different molecular structures in cements blended with 0–50 wt% of a calcined clay (CC) rich in meta illite–smectite. It was found that the water demand of the composite cements increases linerally with the rate of clinker substitution, and that PCE dosages also increase proportionally with the amount of CC, namely approximately doubled at 50% clinker substitution. Among the PCEs, HPEG polymers proved most effective while MPEG and especially IPEG PCEs required higher dosages.

© 2020 The Authors. Published by Elsevier Ltd. This is an open access article under the CC BY-NC-ND license (http://creativecommons.org/licenses/by-nc-nd/4.0/).

1. Introduction

In 2017, the global cement production accounted for ~8% of the total anthropogenic carbon dioxide (CO_2) emission [1]. Approximately 60% of total CO_2 generated in cement manufacturing is mainly due to the decomposition of the raw material calcium carbonate into lime (CaO) followed by the combustion of fossil and secondary fuels to achieve sufficiently high temperatures (~1450 °C) required in the clinkerization process [2,3].

Strategies to reduce CO_2 emission from cement plants include efforts to increase the energy efficiency of the kilns, the use of natural gas as an alternative fuel, and carbon capture and storage (CCS). Additionally, clinker substitution by supplementary

cementitious materials (SCMs) is seen as a key strategy to lower CO_2 emissions from cement [4–10]. However, the limited global availability of traditional SCMs such as fly ash originating from coal-fired power plants or ground granulated blast furnace slag and silica fume from the iron, steel and alloys industries together with an ever increasing global demand for cement due to continued urbanization necessitates to identify additional ecologically and economically attractive alternatives to current cement clinker substitutes. Therefore, many research activities are conducted globally with the aim to develop new binder materials where cement is partially or completely replaced.

In this respect, thermally activated (calcined) clays present an outstanding option as SCM [10] as they are worldwide accessible in essentially unlimited quantity [11,12]. So far, extensive investigations were conducted on different clay minerals concerning suitable calcination temperatures and their pozzolanic activity [13]. Especially kaolinite was studied in much detail [14–16]. More recently, limestone calcined clay blended cement (LC^3) consisting of 50 wt% clinker, 30 wt% calcined clay, 15 wt% limestone and 5 wt% gypsum was proposed for large-scale application and successful construction projects applying this binder have been reported from Cuba and India [17–22]. A characteristic of the LC^3 binder is that the starting clay is suggested to contain about 40 wt% of kaolinite in order to achieve sufficiently high early strength owed to the particular fineness of meta-kaolinite. Unfortunately, natural clay deposits exhibiting such high contents of kaolinite are not always locally available to all cement and concrete producers.

Therefore, other naturally occurring mixed clay minerals (i. e. quartzous clay containing various kinds of clay minerals such as kaolinite, illite, chlorite and montmorillonite, and other accessory minerals and natural deposits such as marl) came into focus as these materials are widely accessible, do not require purification steps and most often are not used in other industrial processes and consequently low-priced [23–25].

Initial studies indicated that the presence of CC in blended cements can significantly increase the water demand [17,26], thus highlighting the fact that in more sophisticated applications, superplasticizers will play a key role to ensure applicability of such low CO_2 binders involving CC. However, so far only few reports have been published on the behavior of PCEs and other superplasticizers in CC blended cements.

For example, Ferreiro et al. found that a calcined kaolin clay requires much more water compared to a thermally activated 2:1 clay (e.g. illite or smectite) when using typical dosages of commercially available PCE superplasticizers, and that the addition of fly ash can significantly improve the rheology of such binders [27]. Moreover, Akbulut et al. reported that specific MPEG PCEs modified with a sulfonated monomer (AMPS) performed well in the LC^3 cement [28], however the dosages required were significantly higher than what the industry is currently used to (up to 0.7%). Such limited literature suggests that a more comprehensive and systematic investigation on the performance of the different kinds of PCEs currently available on the market in CC blended cements is highly needed.

Thus, the objective of this study was to elucidate the dispersing performance of three different kinds of PCEs and their robustness against varying amounts of CC in a blended cement holding up to 50 wt% CC.

First, the impact of increased amounts of CC on the water demand of the blended cement (no PCE present) was evaluated. Next, the dispersing effectiveness of methacrylate ester (MPEG PCE), isoprenol ether (IPEG PCE) and methallyl ether (HPEG PCE) based polycarboxylate copolymers was evaluated in cement pastes where by 0–50 wt% of the clinker were substituted by CC. Those PCEs were selected because MPEG PCEs still dominate the European market whereas IPEG and especially HPEG PCEs are most popular in Asia. Moreover, the impact of different side chain lengths and anionic charge densities present in the PCEs was investigated. Finally, to uncover the interaction mechanism of PCEs possessing varied molecular structures, adsorption measurements were carried out to explain potential differences in their dispersing effectiveness.

The overall aim was to provide insight into the general applicability of PCE-based superplasticizers for CC blended cements, to identify the most suitable PCE chemistry and structural design, and to provide an idea on how much of the targeted CO_2 reduction originating from the clinker substitution will be compromised by higher PCE dosages required in such CC blended composite cements.

2. Materials and methods

2.1. Characterization of materials

2.1.1. Cement

An ordinary Portland cement (OPC) sample CEM I 42.5 R (Schwenk Zement KG, Allmendingen plant, Germany) was used in this study. The phase composition (Table 1) was obtained *via* quantitative powder X-ray diffraction analysis (Q-XRD) (Bruker AXS D8 Advance, Karlsruhe, Germany) using *Rietveld* refinement, *via* thermogravimetric analysis (Netzsch STA 409 TG-MS, Selb, Germany) for the sulfate carriers and according to the *Franke* method [29] for the quantification of free lime.

The average particle size (d_{50} value) measured by laser granulometry (Cilas 1064, Quantachrome GmbH, Odelzhausen, Germany) was 19.8 μm. The specific surface area measured in accordance with DIN EN 196-6 [30] was 3020 cm^2/g while according to the BET method (SA-9601 MP, Horiba Instruments Inc., Kyoto, Japan) a value of 10,000 cm^2/g was found. A density of 3.15 g/cm^3 was determined by helium pycnometry (Ultrapycnometer 1000, Quantachrome Instruments, Boynton Beach, USA).

2.1.2. Raw clay

The raw clay sample used was a naturally occurring Amaltheen clay quarried from the black jura in Bavaria (Germany). The mineralogical composition as determined *via* Q-XRD (Empyrean PANalytical, Almelo, the Netherlands) is shown in Table 2. This clay was low in kaolinite content (~23 wt%), rich in illite–smectite (~32 wt%) and contained other components such as quartz and limestone up to approximately 30 wt%. Prior to calcination it was crushed to a maximum particle size of 10 cm.

The raw clay sample was thermally activated (calcined) for about 30 min at 750 °C in an industrial rotary kiln normally used for the production of expanded clay ("Blähton") applied in thermal insulation renders. Thereafter, the calcined granules were crushed to a maximum particle size of 4 cm and then ground in a roller mill until a d_{50} value of 13.2 μm was reached while the OPC sample exhibited a d_{50} value of 19.8 μm. The particle size distribution of the CC and OPC are presented in Fig. 1.

Table 1
Phase composition of the CEM I 42.5 R sample, as determined *via* Q-XRD using *Rietveld* refinement and thermogravimetry.

Phase	[wt%]
C_3S, m	57.4
C_2S, m	15.2
C_3A, c	5.7
C_3A, o	1.8
C_4AF, o	9.5
Free lime (*Franke*)	0.8
Periclase	0.6
Anhydrite	2.3
Gypsum*	2.3
Dihydrate*	0.3
Calcite	2.6
Quartz	0.4
Dolomite	1.1
Total	100.0

*Determined *via* thermogravimetry.

Table 2
Mineralogical composition of the clay sample before and after calcination, as determined *via* Q-XRD using *Rietveld* refinement.

Mineral phase	Raw clay [wt%]	Calcined clay [wt%]
Kaolinite	22.6	–
Illite-smectite	31.8	4.6
Muscovite	4.7	2.2
Chlorite	5.6	0.4
Quartz	20.0	16.2
Feldspars (albite, anorthite, microcline, orthoclase)	3.8	6.0
Carbonates (calcite, dolomite)	8.5	0.6
Sulfates	–	1.6
Secondary silicates (mullite, hercynite, gehlenite, ringwoodite, diopsite, epidote)	–	6.3
Anatase	1.8	–
Rutile	0.3	–
Hematite	–	0.6
Ore (maghemite, pyrite, magnetite)	0.9	1.1
X-ray amorphous	–	60.8
Total	100.0	100.4
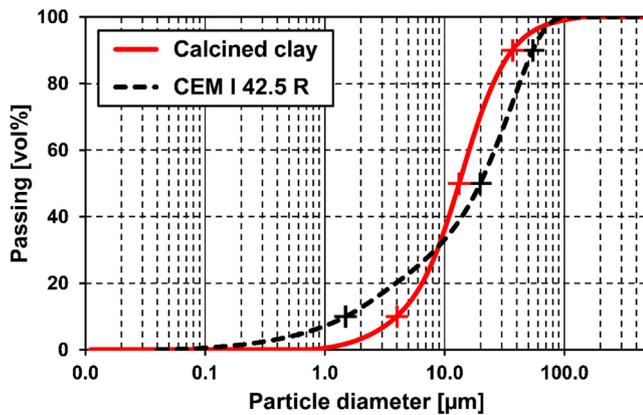
Fig. 1. Particle size distribution of the calcined clay and the CEM I 42.5 R samples.

The density of the calcined clay as determined *via* helium pycnometry was 2.63 g/cm^3 (OPC: 3.15 g/cm^3), while its specific surface area (BET method) was found at 39,000 cm^2/g versus 10,000 cm^2/g for the OPC sample.

The oxide composition of the calcined clay sample was assessed by X-ray fluorescence analysis (Axios, PANalytical, Almelo, the Netherlands) as summarized in Table 3.

The thermal analysis was carried on a Netzsch STA 409 TG-MS (Selb, Germany) instrument over a temperature range from 35 to 1000 °C at a heating rate of 10 °C/min.

A calcination temperature of 750 °C was selected because under this condition, major dehydroxylation of the clay had occurred, as suggested by thermal analysis (see Fig. 2). Moreover, the highest concentrations of dissolved aluminum and silicon ions in the pore solution of CC dispersed in 10 wt% NaOH were found after such treatment which indicates high pozzolanic activity [36,37].

Table 3
Oxide composition of the calcined clay sample, as determined *via* XRF.

Oxide	[wt.%]
SiO$_2$	52.6
Al$_2$O$_3$	22.2
CaO	5.7
Fe$_2$O$_3$	8.4
MgO	2.2
K$_2$O	2.8
Na$_2$O	0.3
SO$_3$	1.4
TiO$_2$	1.0
Loss on ignition (LOI)	2.9
Total	99.5

Generally, dehydroxylation of the raw clay during thermal treatment can be tracked *via* mass loss and occurring endothermic reactions (see Fig. 2). Here, the first peak at 491 °C indicates the dehydroxylation of kaolinite [13,38,39] followed by partial dehydroxylation of the interstratified 2:1 clay minerals (illite–smectite and muscovite) at around 713 °C [16,40]. Beyond this temperature, a mass loss attributed to CO$_2$ release from partial decarbonation of calcite was recorded.

The mineralogical composition of the calcined clay sample is shown in Table 2. As can be seen there, it contains about 61 wt% of amorphous components attributed to the meta clays formed during calcination.

Moreover, Fig. 3 illustrates the XRD patterns of the clay before and after calcination. As the kaolinite diffraction peak is no longer present in the CC sample it can be concluded that kaolinite was completely converted to its amorphous form, meta-kaolinite. Similar observations were made for the phyllosilicate chlorite. However, illite and smectite were not completely decomposed to the amorphous state. Around 27% of their initial content still remained in their crystalline form after thermal treatment at 750 °C, as is shown in Table 2. Also from muscovite, only about 50% of its initial content of 4.7 wt% in the raw clay were dehydroxylated.

From this calcination process a highly amorphous meta clay with significant pozzolanic reactivity was achieved. This material was investigated further with respect to its impact on the water demand of OPC/CC blends and its behavior in the presence of PCE superplasticizers.

2.1.3. PCE dispersants

As superplasticizers, a series of MPEG, IPEG and HPEG PCEs possessing different side chain lengths was employed. All PCE samples except for the HPEG PCEs which were commercial products were self-synthesized *via* free radical co-polymerization. It is noteworthy that this kind of PCEs can be found in common industrial products and are widely available on the market. Furthermore, those PCEs were selected because MPEG PCEs still dominate the European market whereas IPEG and especially HPEG PCEs are most popular and successful on the Asian market.

The MPEG-based polycarboxylates consisting of ω-methoxy poly (ethylene glycol) methacrylate ester macromonomer (n_{EO} = 23, 45; Clariant Produkte Deutschland GmbH, Burgkirchen, Germany) and methacrylic acid (Merck KGaA, Darmstadt, Germany) were prepared as described in [31] while the IPEG PCEs were polymerized from isoprenyl oxy poly(ethylene glycol) macromonomer (n_{EO} = 25 from Clariant Produkte, Burgkirchen, Germany and n_{EO} = 52 from Jilin Zhongxin Chemical Group Co., Ltd., Jilin, China) and acrylic acid (BASF SE, Ludwigshafen, Germany) as presented in [32]. For the HPEG-based PCEs, two commercial products, one possessing a low (ready-mix type) and one of high (precast type) anionic charge density, were employed. The general chemical structures of the three different kinds of PCEs are displayed in Fig. 4.

Molecular properties of all PCE polymers including weight-average molecular masses (M_w), number-average molecular masses (M_n) and their polydispersity index (PDI) were determined *via* gel permeation chromatography (GPC) on a Waters 2695 separation module equipped with three Ultrahydrogel™ columns (120, 250, 500) and an Ultrahydrogel™ guard column (Waters, Eschborn, Germany) using 0.1 N NaNO$_3$ (pH = 12, adjusted with sodium hydroxide) as eluent (flow rate = 1.0 mL/min). A refractive index detector (model 2414, Waters, Eschborn, Germany) and a three angle light scattering detector (Dawn EOS from Wyatt Technology, Santa Barbara, CA/USA) were employed for the identification of the polymer fractions. The value of *dn/dc* used to calculate the absolute molar masses was 0.135 mL/g (value for polyethylene oxide) [33]. The characteristic properties of the PCE samples as obtained from this analysis are summarized in Table 4. The GPC spectra of all PCE samples investigated in this study are presented in Fig. 5. In all spectra, the main peak area represents the PCE fraction while the minor peaks can be attributed to residual macromonomer (MM), poly(acrylic acid) (PAA) and poly(methacrylic acid) (PMAA) homopolymers respectively, and salt and water from the solvent.

The relatively narrow PDI values of 1.8–2.3 indicate that quite uniform polymers have been achieved in the synthesis, thus a selective influence of specific polymer fractions on the dispersing performance can be neglected. Additionally, macromonomer conversion rates above 84% for all PCEs suggest a high yield of copolymer and a rather complete incorporation of the macromonomer into the copolymer.

2.2. Methodologies

2.2.1. Water demand

In order to evaluate the water demand of the cement samples exhibiting increasing contents of calcined clay, modified "mini slump" tests according to DIN EN 1015-3 [34] were performed at a temperature of 20 ± 2 °C and 40 ± 2% relative humidity. The water-to-binder (w/b) ratio was adjusted to obtain a target slump flow of 18.0 ± 0.5 cm. These w/b values were determined in blends with cement substitution rates from 0 to 50 wt% at incremental steps of 10 wt%, and for the calcined clay. From the differences in w/b ratio of individual OPC/CC blends their water demand could be assessed.

The tests were conducted as follows: In a porcelain cup, 300 g of binder were added within one minute to deionized water or (in the case of CC) to synthetic cement pore solution (SCPS), allowed to soak for one minute and then mixed manually for two minutes with a spoon. Immediately thereafter, the cement paste was
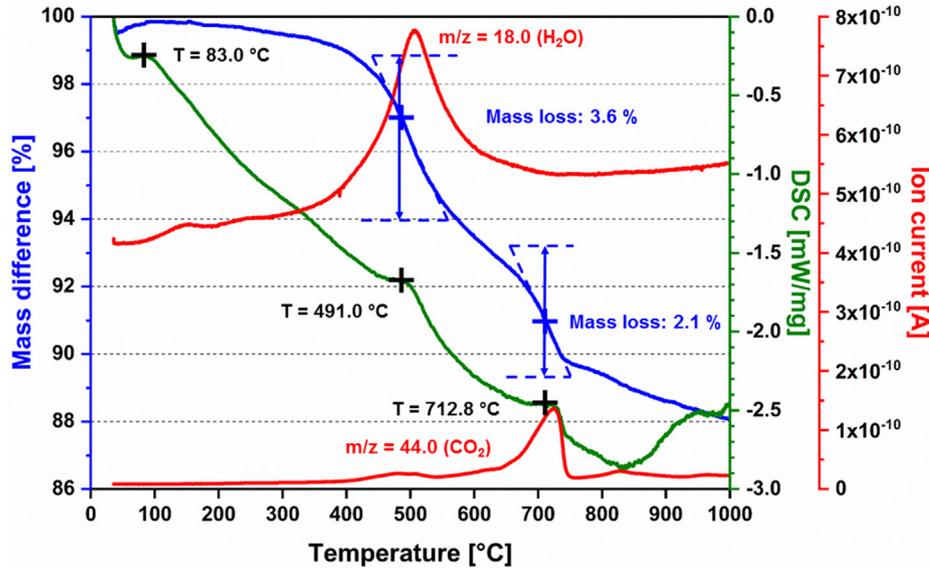
Fig. 2. Thermogravimetric analysis of the raw clay sample used to select the calcination temperature.
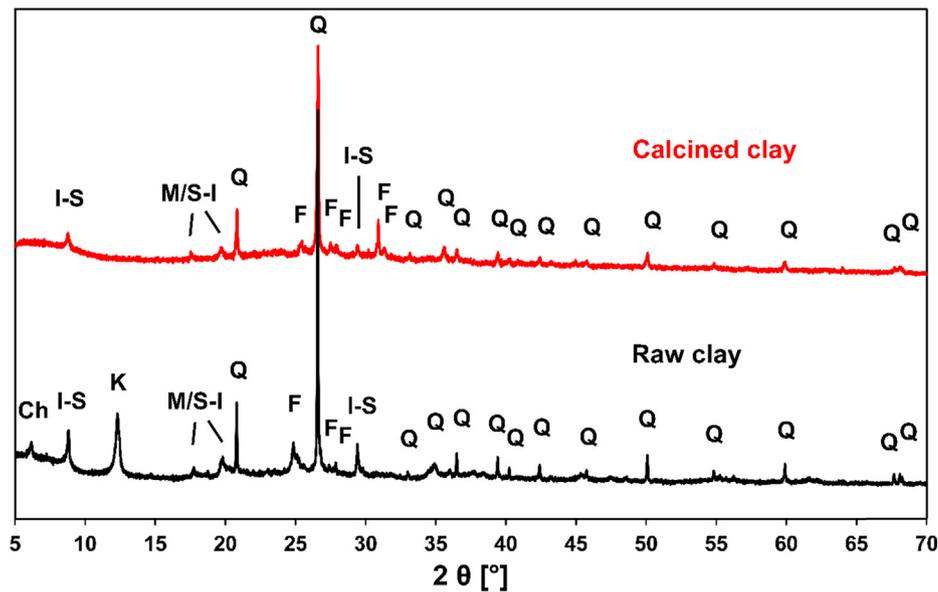

Fig. 3. Powder XRD patterns of the raw and the calcined clay sample (Ch = chlorite, F = feldspar, I-S = illite–smectite, K = kaolinite, M = muscovite, Q = quartz).

poured into a *Vicat* cone (height 4.0 cm, bottom diameter 8.0 cm and top diameter 7.0 cm) placed on a glass plate and filled to the brim. The cone was removed vertically and the diameter of the resulting paste spread was measured twice with a caliper, the second measurement being perpendicular to the first, and averaged to obtain the spread flow value. Each test was performed three times, the average of the paste flow diameter from each individual experiment giving the final slump flow value.

The SCPS used as dispersing medium for the calcined clay resembled the pore solution of an ordinary Portland cement with a pH of 12.9. The SCPS was prepared as described in [35] by solving 1.72 g of $CaSO_4 \cdot 2H_2O$, 6.959 g of Na_2SO_4, 4.757 g of K_2SO_4, and 7.12 g of KOH in 1 L of deionized water.

2.2.2. Dispersing performance

The dispersing performance of superplasticizers was assessed by measuring the paste flow in accordance to the "mini slump" test outlined above. However, the w/b ratio was fixed at 0.50 in order to simulate conditions which are relevant for practical application. PCE superplasticizers were initially dissolved in the mixing water (either deionized water or SCPS) and PCE dosages were varied to achieve a paste spread of 26.0 ± 0.5 cm.

2.2.3. Adsorption measurements

The dosage dependent adsorbed amounts of MPEG-PCEs on OPC and calcined clay were determined using the depletion method. For each PCE dosage (i.e. from 0.1 to 2.0% by weight of binder, % bwob), the amount remaining non-adsorbed in the pore solution was quantified by measuring the total organic carbon (TOC) content of the cement or calcined clay pastes admixed with the appropriate amount of superplasticizer. In a typical experiment, 16 g of binder were added to 8.0 g of deionized water or SCPS (w/b = 0.50) holding the corresponding amount of pre-dissolved PCE, then homogenized for two minutes with a vortex mixer (VWR International, 248 Radnor, USA) at 2400 rpm and centrifuged for ten minutes at 8500 rpm (Biofuge, Primo R, 249 Heraeus, Hanau, Germany). The supernatant was collected, filtered through a 0.2 µm syringe filter and acidified in 0.1 M HCl to remove inorganic carbonates and to prevent carbonation of the alkaline solution. For quantification of the organic carbon in the filtrate samples, a LiquiTOC-II analyser (Elementar Analysensysteme GmbH, Hanau, Germany) was used. Each measurement was performed twice. The averaged values were corrected by the blank TOC value found for the cement and calcined clay pastes prepared without PCE. Finally, the adsorbed amount of PCE was calculated from the difference between the TOC content determined in the supernatant and the initial PCE concentration dissolved in the mixing water.
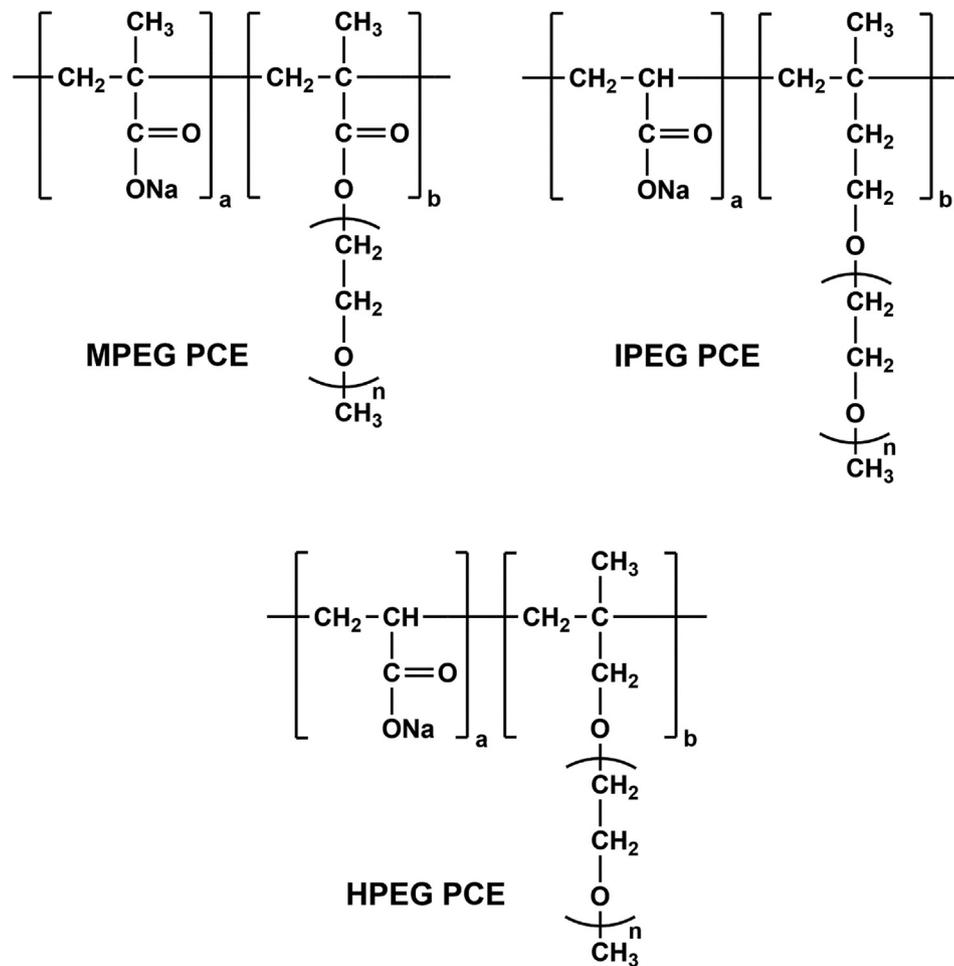
Fig. 4. Chemical structures of the three different kinds of PCE used in the study.

Table 4
Molecular masses (M_w, M_n), polydispersity index (PDI) and macromonomer conversion of the PCE samples used in the study.

Polymer sample	a:b*	n**	M_w (g/mol)	M_n (g/mol)	PDI (M_w/M_n)	Conversion [%]
23MPEG2	2:1	23	32,300	15,500	2.1	85.2
23MPEG6	6:1	23	21,000	10,600	2.0	89.7
45MPEG2	2:1	45	26,700	14,400	1.9	85.6
45MPEG6	6:1	45	27,400	14,000	2.0	86.1
25IPEG6	6:1	25	20,600	10,500	2.0	84.1
52IPEG6	6:1	52	31,500	13,700	2.3	85.5
HPEG precast	–	–	35,800	20,100	1.8	92.3
HPEG ready-mix	–	–	39,800	21,200	1.9	88.6

* a:b represents the molar ratio between (meth)acrylic acid and the macromonomer; ** n represents the number of ethylene oxide units present in the PCE side chain.

3. Results and discussion

3.1. Water demand of CC blended cements

The water demand of OPC/CC blends with different cement substitution rates was assessed by determining the w/b ratio required to achieve a spread flow of 18.0 ± 0.5 cm.

As displayed in Fig. 6, stepwise substitution of the cement by CC prompts a steady increase of the water demand (~7% for every 10 wt % of calcined clay added). For example, at a cement substitution of 50 wt% the w/b ratio had increased by as much as 35% (from 0.48 to 0.65). The increase in the water demand is linear (R^2 = 0.9974), as is shown in Fig. 6. This behavior already implies that higher clinker substitution by CC will provoke higher superplasticizer dosages to achieve the same workability as for the control (OPC). Interest-ingly, the calcined clay sample dispersed in SCPS required a w/b ratio as high as 0.77 (value not shown in Fig. 6), representing a 60% increase in water demand compared to the control.

3.2. Dispersing performance of the PCE samples

In the following, the dispersing performance of the synthesized MPEG, IPEG and HPEG PCEs in control OPC, in calcined clay blended cements of different cement substitution rates and in CC will be presented.

3.2.1. MPEG PCEs

From this kind of PCE, four different samples distinguished by their individual molar ratio between methacrylic acid and the side chain bearing macromonomer (either 2:1 or 6:1) or by the length
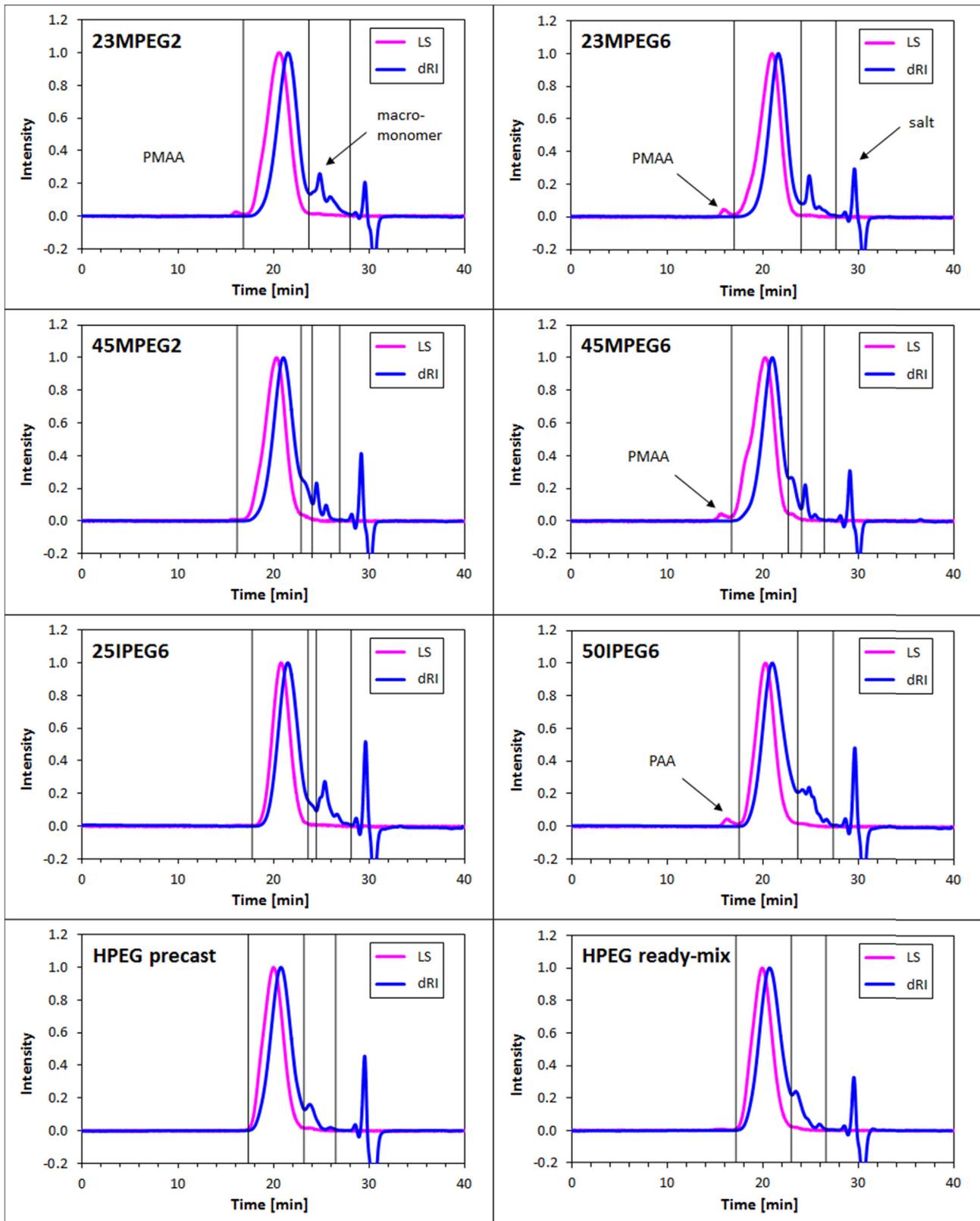
Fig. 5. GPC spectra of all PCE polymer samples used in the study.

of the side chain (either 23 or 45 ethylene oxide units), thus expressing various structural motifs, were compared. The results obtained are presented in Fig. 7.

First, it is observed that for MPEG PCEs holding a short side chain (n_{EO} = 23), a molar composition of 2:1 (MAA:-macromonomer) yields a product which is more effective than a
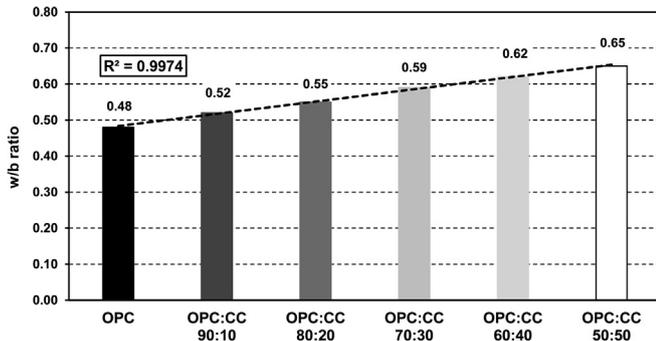
Fig. 6. W/b ratio to yield a paste spread flow of 18.0 ± 0.5 cm for OPC iteratively blended with calcined clay.

copolymer of high anionic character derived from a molar ratio of 6:1. However, when the length of the side chain is increased to 45 EO units, then this relationship becomes reversed, i.e. the polymer composed of a molar ratio of 6:1 provides better dispersing performance. Thus, optimal effectiveness can be achieved from MPEG PCEs possessing shorter (n_{EO} = 23) or longer side chains (n_{EO} = 45), however in both cases the anionicity of the molecules needs to be modulated. Thus, 23MPEG2 (lower anionic species) and 45MPEG6 (higher anionic species) perform superior while the copolymers 23MPEG6 and 45MPEG2 require higher dosages across all OPC/CC blends.

Furthermore, it is detected that increasing contents of CC in the blended cements generally result in steadily ascending PCE dosages, with an increase of about 130% from control OPC to the 50:50 blend of OPC/CC. As expected, the CC by its own demands even higher PCE dosages, and here, independent of side chain length the more anionic polymer samples 23MPEG6 and 45MPEG6 vastly outperform their less anionic counterparts 23MPEG2 or 45MPEG2 which can barely fluidize this binder.

The results allow to conclude that at higher substitution rates of OPC by CC, a different molecular species than that optimal for OPC becomes more preferable. While MPEG PCEs exhibiting medium long side chains (n_{EO} = 23) and low anionicity are most effective, in OPC and at low clinker substitution rates (up to 20% replacement) MPEG PCEs of longer side chain (45 EO units) and higher anionic character (molar ratio 6:1) work better in blended cements of >20% cement substitution.

3.2.2. IPEG PCEs

IPEG PCEs possessing different side chain lengths (either 25 or 50 EO units), but the same high acid content (molar ratio of 6:1) were probed.

As presented in Fig. 8, this kind of PCE generally is inferior to the MPEG PCEs. Unlike MPEG, IPEG with a longer side chain (50 EO units) always outperforms the polymer exhibiting a medium long side chain (25 EO units).

However, this kind of PCE stands out in that it is particularly effective in the dispersion of the calcined clay, thus suggesting a more favorable interaction between this kind of PCE and CC.

3.2.3. HPEG PCEs

Two commercial standard HPEG PCE products were studied. They are distinguished by their anionicity, a highly anionic PCE mostly applied in precast concrete and the other a less anionic, hydrolysable slump-retainer kind which is predominantly used in the ready-mix concrete industry.

The results exhibited in Fig. 9 clearly indicate that this kind of PCE is the most effective PCE among those investigated. They produce a superior performance across all previously tested PCE samples in OPC, OPC/CC blends and even in the CC, and to a higher extent for the precast type. These data are most encouraging because they confirm that currently available PCE technology can handle such CC blended cements at reasonably low addition rates. Still, for the most effective PCE, the dosage increases by no less than 80% from OPC to the 50:50 blend of OPC/CC, as recorded for the precast product in Fig. 9.

Moreover, it was found that the HPEG-based precast kind presents the most effective superplasticizer also in neat CC (dosage value 0.13% bwob vs. 0.18% bwob for 45MPEG6 and 0.20% bwob for 50IPEG6). This further underlines the overall superiority of HPEG PCEs among the PCE products.

3.2.4. Summary of PCE performances

The differences with respect to the tolerance of higher CC contents by the individual types of PCEs investigated is illustrated in Fig. 10. There, the PCE dosages were plotted against the clinker substitution rate, and the ascension of the dosage curves was calculated. From this it was found that both HPEG PCEs were most robust towards higher CC contents whereas both IPEG PCEs and 23MPEG6 exhibited the lowest tolerance to interground CC. The values shown in the legend of Fig. 10 represent the slopes for linear trendlines. From this data it can be seen that HPEG exhibits the lowest slope when increasing the calcined clay content, and therefore presents the most robust superplasticizer in these CC blended cements.

3.3. Adsorption of MPEG PCEs

To better understand the different behaviors of the PCE samples recorded before, adsorption measurements on OPC and CC respec-
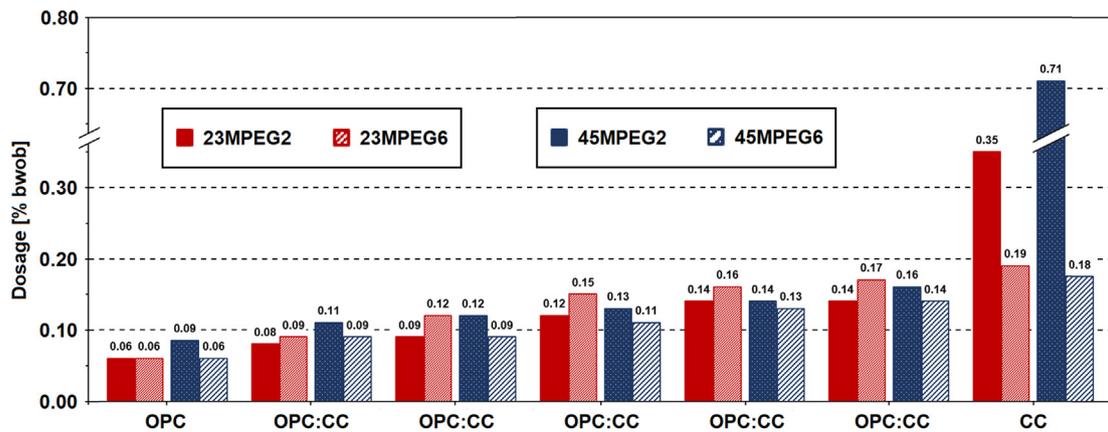

Fig. 7. Dosages of individual MPEG PCE samples required to achieve a paste spread of 26 ± 0.5 cm; w/b ratio fixed at 0.5.
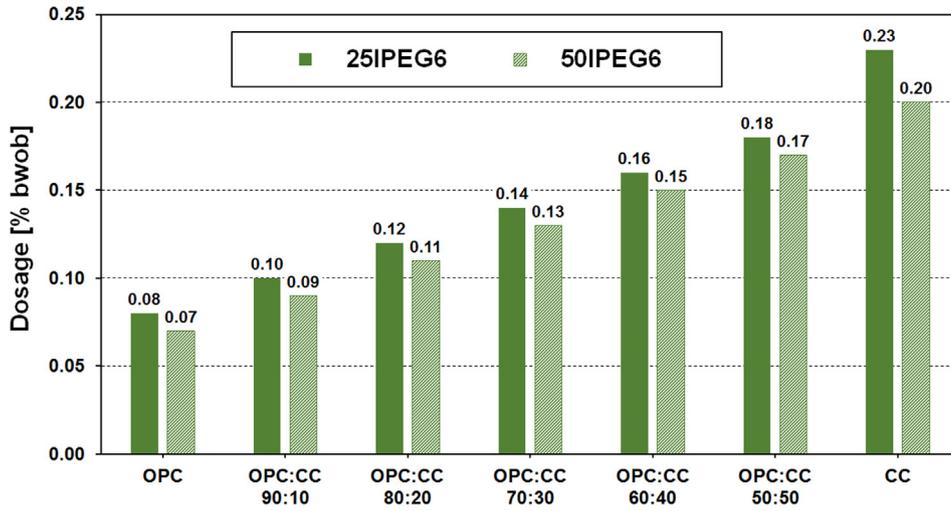
Fig. 8. Dosages of IPEG PCE samples possessing different side chain lengths required to achieve a paste spread of 26.0 ± 0.5 cm; w/b ratio fixed at 0.5.
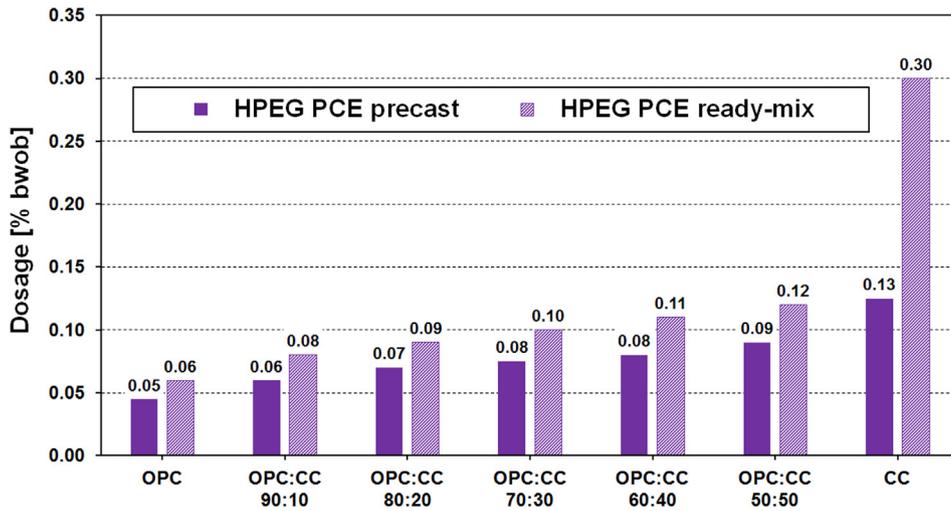

Fig. 9. Dosages of HPEG type PCE samples required to achieve a paste spread of 26.0 ± 0.5 cm; w/b ratio fixed at 0.5.
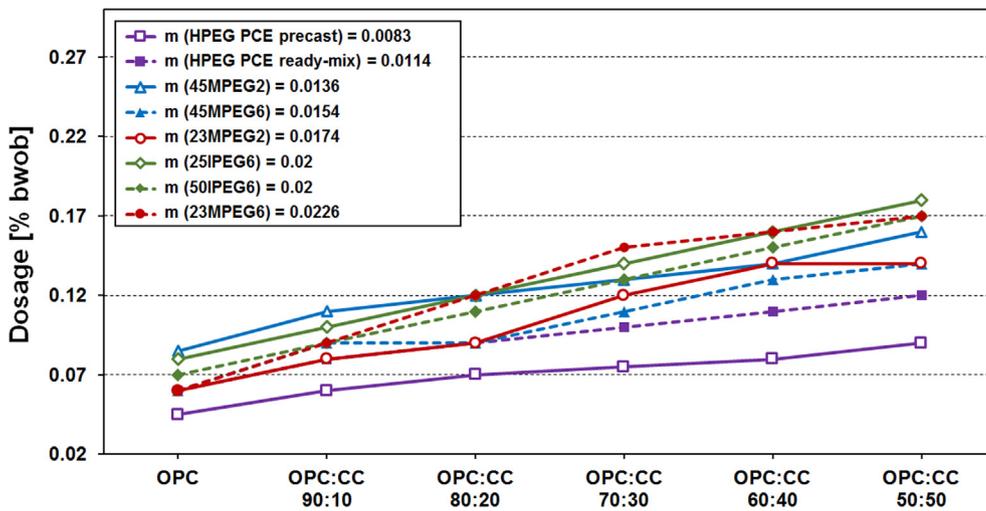

Fig. 10. Development of dosage for different kinds of PCEs at increasing clinker substitution rates in pastes to reach a spread flow of 26.0 ± 0.5 cm; w/b ratio fixed at 0.5.

tively were performed for the series of MPEG PCEs. The results are displayed in Fig. 11. The MPEG PCEs were selected for this mechanistic study because of their greater diversity in molecular composition.

There, it can be seen that the PCE samples exhibiting higher anionicity (prepared from a molar ratio of acid:side chain of 6:1) consistently adsorb in higher amounts, compared to their less anionic counterparts synthesized at a molar ratio of 2:1. This effect is independent of the side chain length (23 or 45 EO units). Furthermore, the highly anionic polymers always adsorb in higher amounts on OPC than on CC at the saturation point. Interestingly, a different behavior was recorded for the less anionic species which produce quite comparable adsorbed amounts on both OPC and CC.

Moreover, the curves presented in Fig. 11 also suggest that at PCE dosages which are commonly applied in actual concrete (≤0.2% bwob) and which have been shown to be applicable also in the CC blended cements (see Figs. 7–9), the adsorbed amounts on OPC and CC are essentially the same. Apparently, the discrepancy between these adsorption experiments and the fact that in the "mini slump" tests different PCE dosages are required when OPC or CC are used can be attributed to the different mixing protocols performed in both tests.

Thus, it is obvious that the interaction of PCEs with cements containing CCs is not well understood at present and that significant additional research is needed in this field. Especially the different kinds of meta clays which can be present in CCs should be taken into account.

4. Conclusion

The influence of three different types of PCE-based superplasticizers on the fluidity of composite cements containing up to 50 wt % of a calcined clay as SCM was investigated.

A natural German mixed layer clay rich in illite and smectite and low in kaolinite was calcined at 750 °C for this study.
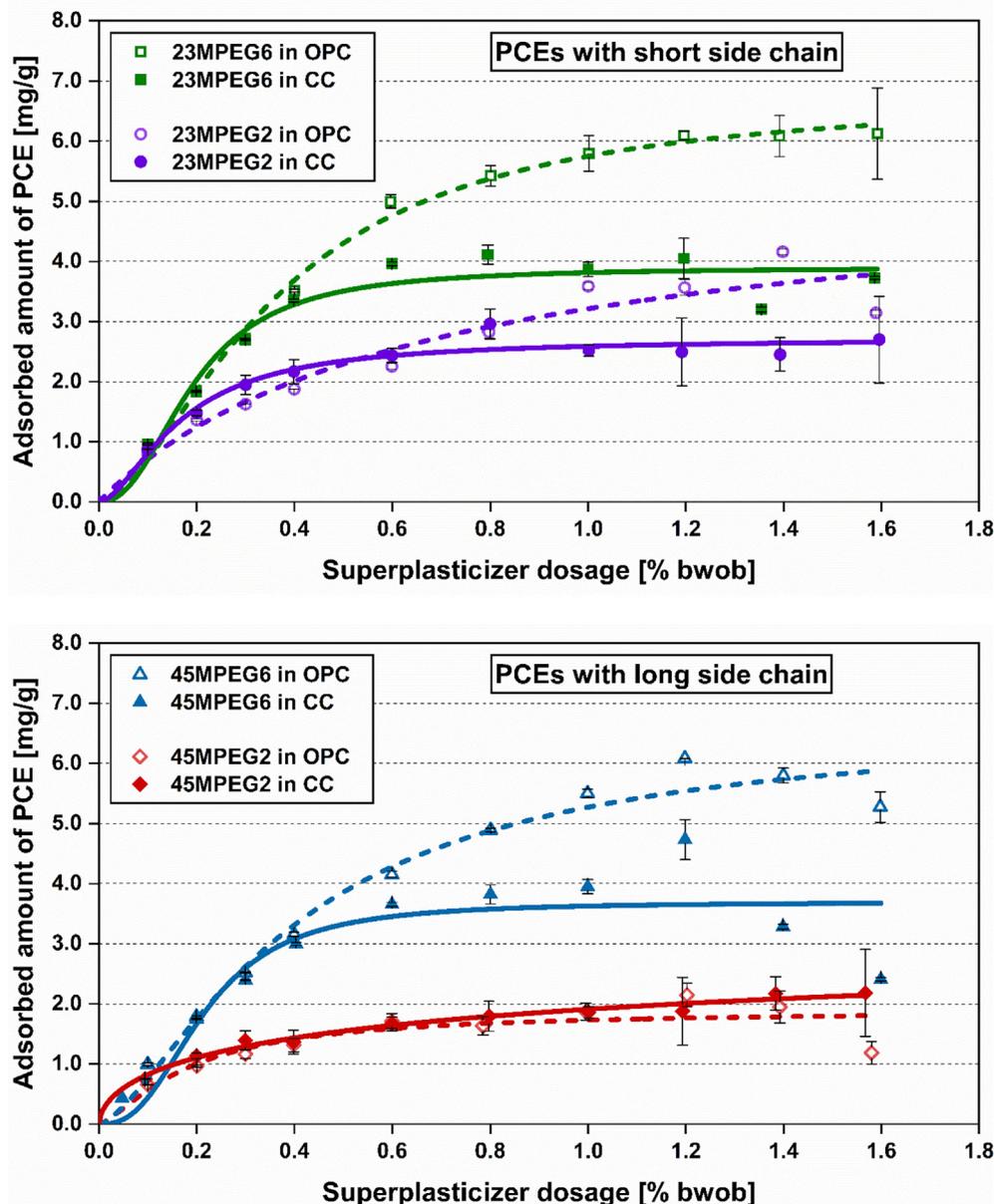

Fig. 11. Dosage-dependent adsorbed amounts of four MPEG PCEs on OPC and CC, as determined *via* TOC measurement; top: PCEs with short side chain (n_{EO} = 23); bottom: PCEs with long side chain (n_{EO} = 45).

M. Schmid, J. Plank / Construction and Building Materials 258 (2020) 119576

As best performing superplasticizers, conventional, commercially available HPEG type PCEs of high anionic charge density and exhibiting side chains made of 50 ethylene oxide units were identified. Also, MPEG PCEs possessing shorter side chains and low acid content were found to be quite effective superplasticizers.

Generally, PCE dosages increased with ascending content of calcined clay to satisfy its higher water demand and its more pronounced uptake of PCE as compared to OPC. As a rule of thumb, the increase amounts to about 100% when migrating from control OPC to a 50:50 blend of OPC and CC. Consequently, some of the ecological advantage of OPC/CC blends is lost, because the raw material production, synthesis, transportation etc. of this admixture also comes with some CO_2 emission.

Similar as in OPC, the dispersing effectiveness of PCEs in calcined clay blended cements with high substitution rates (e.g. 30 wt%) increases with longer side chain of the macromonomer and a more pronounced anionic character.

Most important, however, is the finding that PCEs which are currently available on the market and present industrial benchmark products can well handle such additions of calcined clay. This emphasizes the feasibility of using thermally activated clays as SCMs in composite cements.

In future studies, the workability (= "slump") retaining properties of ready-mix concrete type PCEs and the influence of the PCEs on the early strength development (pozzolanic reaction) of the composite binder should be investigated because in fact by far most of the PCEs are applied in this kind of concrete. Finally, the findings of this study should be extended to other kinds of calcined clays, e.g. those particularly rich in meta-kaolinite, as is the case in the LC[3] binder.

CRediT authorship contribution statement

Marlene Schmid: Conceptualization, Data curation, Project administration, Validation, Visualization, Writing - original draft, Writing - review & editing. **Johann Plank:** Conceptualization, Project administration, Supervision, Validation, Writing - original draft, Writing - review & editing.

Declaration of Competing Interest

The authors declare that they have no known competing financial interests or personal relationships that could have appeared to influence the work reported in this paper.

Acknowledgments

References

[1] P.J.M. Monteiro, S.A. Miller, A. Horvath, Towards sustainable concrete, Nat. Mater. 16 (2017) 698–699.

[2] R.M. Andrew, Global CO_2 emissions from cement production, Earth Syst. Sci. Data 10 (2018) 195–217.

[3] E. Worrell, L. Price, N. Martin, C. Hendriks, L.O. Meida, Carbon dioxide emissions from the global cement industry, Annu. Rev. Energy Env. 26 (2001) 303–329.

[4] K.L. Scrivener, V.M. John, E.M. Gartner, Eco-efficient cements: potential economically viable solutions for a low-CO_2 cement-based materials industry, Cem. Concr. Res. 114 (2018) 2–26.

[5] M. Schneider, Process technology for efficient and sustainable cement production, Cem. Concr. Res. 78 (2015) 14–23.

[6] H.-M. Ludwig, W. Zhang, Research review of cement clinker chemistry, Cem. Concr. Res. 78 (2015) 24–37.

[7] E. Gartner, H. Hirao, A review of alternative approaches to the reduction of CO_2 emissions associated with the manufacture of the binder phase in concrete, Cem. Concr. Res. 78 (2015) 126–142.

[8] R. Rosković, D. Bjegović, Role of mineral additions in reducing CO_2 emission, Cem. Concr. Res. 35 (2005) 974–978.

[9] D.J. Barker, S.A. Turner, P.A. Napier-Moore, M. Clark, J.E. Davison, CO_2 capture in the cement industry, Energy Procedia 1 (2009) 87–94.

[10] S.A. Miller, Supplementary cementitious materials to mitigate greenhouse gas emissions from concrete: can there be too much of a good thing?, J. Cleaner Prod. 178 (2018) 587–598.

[11] M. Antoni, J. Rossen, F. Martirena, K. Scrivener, Cement substitution by a combination of metakaolin and limestone, Cem. Concr. Res. 42 (2012) 1579–1589.

[12] M. Singh, M. Garg, Reactive pozzolana from Indian clays – their use in cement mortars, Cem. Concr. Res. 36 (2006) 1903–1907.

[13] R. Fernandez, F. Martirena, K.L. Scrivener, The origin of the pozzolanic activity of calcined clay minerals: a comparison between kaolinite, illite and montmorillonite, Cem. Concr. Res. 41 (2011) 113–122.

[14] C. He, E. Makovicky, B. Osbaeck, Thermal stability and pozzolanic activity of calcined kaolin, Appl. Clay Sci. 9 (1994) 165–187.

[15] N. Garg, J. Skibsted, Dissolution kinetics of calcined kaolinite and montmorillonite in alkaline conditions: evidence for reactive Al(V) sites, J. Am. Ceram. Soc. 102 (2019) 7720–7734.

[16] C. He, E. Makovicky, B. Osbaeck, Thermal stability and pozzolanic activity of calcined illite, Appl. Clay Sci. 9 (1995) 337–354.

[17] K. Scrivener, F. Martirena, S. Bishnoi, S. Maity, Calcined clay limestone cements (LC[3]), Cem. Concr. Res. 114 (2018) 49–56.

[18] Y. Dhandapani, T. Sakthivel, M. Santhanam, R. Gettu, R.G. Pillai, Mechanical properties and durability performance of concretes with Limestone Calcined Clay Cement (LC[3]), Cem. Concr. Res. 107 (2018) 136–151.

[19] F. Martirena, K. Scrivener, Low Carbon Cement LC[3] in Cuba: ways to achieve a sustainable growth of cement production in emerging economies, in: F. Martirena, A. Favier, K. Scrivener (Eds.), 2nd International Conference on Calcined Clays for Sustainable Concrete, Springer Nature, Havana City (Cuba), 2018, pp. 318–321.

[20] G. Esperanza, I. Machado-Lopez, J.F. Martirena-Hernandez, Experimental pilot plant for low carbon cements development: the cuban innovative project, in: J. F. Martirena-Hernández, A. Alujas-Díaz, M. Amador-Hernández (Eds.) Proceedings of the International Conference of Sustainable Production and Use of Cement and Concrete (ICSPCC 2019), Springer Nature Switzerland AG, Villa Clara (Cuba), 2020, pp. 141-147.

[21] S. Bishnoi, S. Maity, Limestone Calcined Clay Cement: the experience in India this far, in: F. Martirena, A. Favier, K. Scrivener (Eds.), 2nd International Conference on Calcined Clays for Sustainable Concrete, Springer Nature, Havana City (Cuba), 2018, pp. 64–68.

[22] A.C. Emmanuel, G. Mishra, S. Bishnoi, Initial performance evaluation of calcined clay based ternary blended cement under various climatic conditions in India, in: F. Martirena, A. Favier, K. Scrivener (Eds.), 2nd International Conference on Calcined Clays for Sustainable Concrete, Springer Nature, Havana City (Cuba), 2018, pp. 160–164.

[23] S.E. Schulze, J. Rickert, Suitability of natural calcined clays as supplementary cementitious material, Cem. Concr. Compos. 95 (2019) 92–97.

[24] T. Danner, G. Norden, H. Justnes, Characterisation of calcined raw clays suitable as supplementary cementitious materials, Appl. Clay Sci. 162 (2018) 391–402.

[25] R. Gmür, K.-C. Thienel, N. Beuntner, Influence of aging conditions upon the properties of calcined clay and its performance as supplementary cementitious material, Cem. Concr. Compos. 72 (2016) 114–124.

[26] N. Beuntner, K. Rapp, K.-C. Thienel, Efficiency of calcined clay in cementitious systems, in: T.C. Holland, P.R. Cupta, V.M. Malhotra (Eds.), 12th International Conference on Recent Advances in Concrete Technology and Sustainability Issues, Sheridan Books, Prague (Czech Republic), 2012, pp. 413–424.

[27] S. Ferreiro, D. Herfort, J.S. Damtoft, Effect of raw clay type, fineness, water-to-cement ratio and fly ash addition on workability and strength performance of calcined clay – Limestone Portland cements, Cem. Concr. Res. 101 (2017) 1–12.

[28] O. Akhlaghi, T. Aytas, B. Tatli, D. Sezer, A. Hodaei, A. Favier, K. Scrivener, Y.Z. Menceloglu, O. Akbulut, Modified poly(carboxylate ether)-based superplasticizer for enhanced flowability of calcined clay-limestone-gypsum blended Portland cement, Cem. Concr. Res. 101 (2017) 114–122.

[29] B. Franke, Bestimmung von Calciumoxyd und Calciumhydroxyd neben wasserfreiem und wasserhaltigem Calciumsilikat, Zeitschrift für anorganische und allgemeine Chemie 247 (1941) 180–184.

[30] DIN EN 196-6, Prüfverfahren für Zement – Teil 6: Bestimmung der Mahlfeinheit (Methods of testing cement – Part 6: Determination of fineness), Beuth-Verlag, Berlin (2018).

[31] J. Plank, K. Pöllmann, N. Zouaoui, P.R. Andres, C. Schaefer, Synthesis and performance of methacrylic ester based polycarboxylate superplasticizers possessing hydroxy terminated poly(ethylene glycol) side chains, Cem. Concr. Res. 38 (2008) 1210–1216.

[32] J. Plank, H. Li, M. Ilg, J. Pickelmann, W. Eisenreich, Y. Yao, Z. Wang, A microstructural analysis of isoprenol ether-based polycarboxylates and the impact of structural motifs on the dispersing effectiveness, Cem. Concr. Res. 84 (2016) 20–29.

[33] M.T.R. Laguna, R. Medrano, M.P. Plana, M.P. Tarazona, Polymer characterization by size-exclusion chromatography with multiple detection, J. Chromatogr. A 919 (2001) 13–19.

[34] DIN EN 1015-3, Prüfverfahren für Mörtel für Mauerwerk – Teil 3: Bestimmung der Konsistenz von Frischmörtel (mit Ausbreittisch), 2007.

[35] A. Habbaba, J. Plank, C. Jantzen, Surface chemistry of ground granulated blast furnace slag in cement pore solution and its impact on the effectiveness of polycarboxylate superplasticizers, J. Am. Ceram. Soc. 95 (2) (2012) 768–775.

[36] R. Sposito, M. Schmid, N. Beuntner, S. Scherb, J. Plank, K.-C. Thienel, Early hydration behavior of blended cementitious systems containing calcined clays and superplasticizer, 15th International Congress on the Chemistry of Cement (ICCC), Prague (Czech Republic), 2019.

[37] S. Scherb, N. Beuntner, K.-C. Thienel, Reaction kinetics of the basic clays present in natural mixed clays, in: F. Martirena, A. Favier, K. Scrivener (Eds.), Calcined Clays for Sustainable Concrete - Proceedings of the 2nd International Conference on Calcined Clays for Sustainable Concrete, Springer Nature, La Havanna (Cuba), 2018, pp. 427-433.

[38] D. Yeskis, A.F. Koster van Groos, S. Guggenheim, The dehydroxylation of kaolinite, Am. Mineral. 70 (1985) 159–164.

[39] E. Gasparini, S.C. Tarantino, P. Ghigna, M.P. Riccardi, E.I. Cedillo-González, C. Siligardi, M. Zema, Thermal dehydroxylation of kaolinite under isothermal conditions, Appl. Clay Sci. 80–81 (2013) 417–425.

[40] E. Mazzucato, G. Artioli, A. Gualtieri, High temperature dehydroxylation of muscovite-2M1: a kinetic study by in situ XRPD, Phys. Chem. Minerals 26 (1999) 375–381.